Chapter VI

An integrated microvessels-on-a-chip platform for automated multi-channel perfusion and continual *in situ* oxygen monitoring

Abidemi Junaid, Raphaël Zwier, Ankur Kislaya, Wendy Stam, Bas Trietsch, Jerry Westerweel, Alireza Mashaghi, Janine van Gils, Anton Jan van Zonneveld, Thomas Hankemeier

Manuscript to be submitted (2020)

Abstract

Organs-on-Chips have recently emerged as a viable system for modelling microvascular diseases and drug screening. These *in vitro* microvascular disease models, featuring biomimetic compositions, architectures and functions found in the human microvessel, are expected to replace the traditional models based on two-dimensional (2D) static cell culture. Since blood flow and shear stress play a significant role in modulating the physiological responses of endothelial cells in the microvessels, incorporation of flow is often essential for microvessels-on-chips to serve as biologically relevant models. Here, we describe the development of a multi-channel microfluidic pumping and *in situ* oxygen monitoring system for the microvessels-on-chips. We performed biochemical assays in the microvessels-on-chips under shear stress and oxygen measurement to validate our system. The morphology and gene expression of the microvessels-on-chips under shear stress were similar to what is found *in vivo* and deviate significantly from shearless models. We believe that our integrated microvessels-on-a-chip platform has paved the way to promote high-throughput perfusion and real-time oxygen measurement in an automated manner for modeling the microvascular system.

Introduction

Heart failure (HF) is the number one cause of death worldwide [1]. In recent years it has become clear that as much as 50% of HF patients show symptoms of HF in the presence of preserved ejection fraction (HFpEF) [2]. Recent studies have identified causal relation between HFpEF and microvascular dysfunction [3, 4]. Therefore, finding ways to treat microvascular dysfunction has become very important in drug discovery. To address this issue, new approaches are required to fill the technology gap needed for effective drug discovery and screening [5].

For decades now, conventional cell culture models have been used to study microvascular diseases. Conventional cell culture models require two-dimensional (2D) cell culturing, static conditions, large working volumes, and recurrent system disturbance. Hence, they fail to reconstitute the *in vivo* cellular dynamic environment and are not suitable for monitoring the microenvironment that can be translated to *in vivo* situation. Organs-on-Chips have recently been proposed to mimic the physiological conditions of the microvessels. These miniaturized human microvessel models have several advantages over conventional models, such as three-dimensional (3D) structure, cell-cell interactions and extracellular matrix (ECM) [6, 7]. Therefore, they have been successfully used to model diseases and study the effects of drugs [8]. Although, many in the field focus on the construction of biomimetic microvessel models, it is now firmly acknowledged that incorporating perfusion and sensors would allow the exertion of mechanical forces on the surface of endothelial cells and *in situ* monitoring the status of the microvessels [9, 10]. Such a need originates from the fact that perfusion trigger the production of proteins and transcription factors that are able to suppress pro-inflammatory signaling pathways and this can be measured online with biosensors [11].

One of the challenges of organs-on-chips is to fabricate functional microvessels that can be integrated with other systems, can withstand continuous perfusion after cell seeding and run in fully automated manner over extended periods of time. This is because commercially available perfusion systems together with sensors are often incompatible with microfluidic systems. However, several efforts have been initiated toward the accomplishment of this goal. For example, prototype organs-on-chips under shear force and with *in situ* sensing capabilities were developed to perfuse endothelial cells with real time monitoring of mechanical microenvironment, record field potential and measure transepithelial electrical resistance

(TEER) [12, 13]. However, these organs-on-chips were built upon a single chip, limited to monitoring of a single microenvironment and with no automation [14].

Here, we report the development of an integrated organ-on-a-chip modular platform that includes a multi-channel micropump for high-throughput perfusion of fluids and a physical sensor for monitoring oxygen in extracellular microenvironment. The oxygen monitoring could be performed *in situ* without interrupting the system. The micropump and oxygen sensor were controlled by LabView in an automated manner. We analyzed the performance of the platform by adapting it to the microvessels-on-chips and carrying out biochemical assays to correlate the phenotype of endothelial cells to the *in vivo* situation. We anticipate that in the future, our platform technology will enable organ-on-a-chip models to achieve automation and *in situ* monitoring of biochemical parameters while being perfused.

Methods

µPIV

PIV is a quantitative method which is commonly used for measuring velocity field in experimental fluid mechanics. This technique measures the velocity of a fluid element indirectly by measuring the displacement of tracer particles within the fluid which must be added prior to the start of the experiment. A high-power light source for the illumination of the tiny tracer particles is required to expose the image sensor of the camera to sufficient scattered light. In micro-scale application, it is generally referred to as µPIV [24, 25]. This measurement was carried out on the rerouted 2-lane in order to calibrate the shear stress of our microfluidic pump. The microfluidic channel has a height of 200 µm and is 400 µm wide. The working fluid is a solution of 2% blood serum (viscosity and density are 1.25 mPa·s and 1.0242 g/mL respectively) dissolved in water. The viscosity of the prepared solution was checked at 37°C using a viscometer (Contraves Low shear 40). The dynamic viscosity was determined for different deflections varying from 80 rad/s to -80 rad/s in steps of 20 rad/s and averaged to get the mean dynamic viscosity of 0.87 mPa.s. The solution was seeded with

monodispersed polystyrene particles with a diameter of 1.046 ± 0.016 µm (Microparticles GmbH).

Images were recorded from LaVision's Imager Intense camera (CCD, 12-bit 1376×1050pixels, pixel pitch 6.4 µm). The camera was mounted on the Nikon eclipse Ti2 inverted microscope equipped with 10x objective lens (Nikon CFI Plan Fluor). The camera exposure time was set at 4000 µs to allow enough light to enter the image sensor for clear identification of the particle images. The acquisition frequency of 9.5 Hz was used to capture the in-plane displacement of 2 pixel between two consecutive recordings. For statistical averaging to reduce the random noise, 3000 images were acquired for each data set. Images were acquired for flow behavior at different pulsatile pump rotational speed between 10 to 100 RPM. Image acquisition and PIV processing are performed with the LaVision DaVis 8.3 software. In PIV processing, for reducing the background image, a time filter is used to subtract the minimum intensity from all images. Followed by taking sequential time-series of the single-pass FFT cross-correlation for all the images. For the velocity field reconstruction, the interrogation windows of 64×64 pixels with 50% overlap was chosen. The microfluidic pump shear stress was derived from the equations:

$$\bar{v}\,(m/s) = \frac{s}{t}$$

$$Q(m^3/s) = A \cdot \bar{v}$$

$$\tau(dyne/cm^2) = \frac{6 \cdot Q \cdot \eta}{w \cdot h^2} \cdot 10$$

where $\bar{v}$ is particle velocity; s is the distance the particle traveled in time t; Q is the volume flow rate, A is the cross-section area of the microfluidic channel; τ is the calculated shear stress; η is the measured viscosity of the media; w and h are the width and height of the channel.

Cell culture

Human umbilical vein endothelial cells (HUVECs) were cultured in Endothelial Cell Growth Medium 2 (C-39216; PromoCell). For all microfluidic cell culture, we used a modified 2-lane

OrganoPlate, rerouted 2-lane, made by MIMETAS with inlets and outlets that are compatible with our microfluidic pump. The microvascular and extracellular matrix (ECM) channels were separated by phaseguides [16]. Before seeding the cells, 4 mg/ml rat tail collagen type 1 (3440-005-01; Trevigen) neutralized with 10% 37 g/L Na_2CO_3 (S5761; Sigma) and 10% 1 M HEPES buffer (15630-056; Gibco) was added in the ECM channels. Subsequently, the collagen was let to polymerize by incubating the device for 10 minutes in the incubator at 37°C and 5% CO_2. The observation windows were filled with 50 µl Hank's Balanced Salt Solution with calcium and magnesium buffers (HBSS+; 24020117; Life Technologies) for optical clarity and to prevent gel dehydration. Using a repeater pipette, 20 µl of 1% gelatin was added into the inlet of each microvascular channel and the device was put in the incubator at 37°C for 30 minutes. Subsequently, the gelatin was replaced with 20 µl of culture media. We trypsinized cells at 80-90% confluency and seeded $15 \cdot 10^6$ cells/ml in the outlet of the microvascular channels of the OrganoPlate. Afterwards, the cells were incubated at 37°C and 5% CO2 for one hour to allow microvascular formation. After incubation, 50 µl of culture medium was added to the inlets and outlets of the microvascular channels. The device was placed on an interval rocker platform (Perfusion rocker, MIMETAS) with a 7° angle of motion and an eight-minute timed operation to allow continuous bidirectional flow of medium in the microvessels. After 48h, the medium was refreshed, and the microvessels were perfused for 24, 48 and 96h with the microfluidic pump for unidirectional flow.

Quantitative RT-PCR

RNA isolation was performed using Buffer RLT lysis buffer (Qiagen) and isolated using Qiagens' RNAeasy kit according to manufactures instructions. Subsequently, lysate of eight microvessels were pooled to form one sample to allow analyses of gene expressions at low concentrations due to low cell numbers. 250 ng of total RNA was used for reverse transcription mediated cDNA synthesis using random and oligo(dT) primers (Bio-Rad) according to the manufacturer's protocols. SYBR Select (Invitrogen) and a Biorad CFX384 were used for qRT-PCR analysis. The primer sequences of target genes used were as follows: *Klf2* (sense), CTACACCAAGAGTTCGCATCTG; *Klf2* (antisense), CCGTGTGCTTTCGGTAGTG; *Klf4* (sense), TCAACCTGGCGGACATCAAC; *Klf4* (antisense), AGCACGAACTTGCCCATCA; *18S rRNA* (sense), GGATGTAAAGGATGGAAAATACA; *18S rRNA* (antisense), TCCAGGTCTTCACGGAGCTTGTT.

Levels of expression were normalized to *18S rRNA* and quantified using the comparative cycle threshold (ΔΔCt) method.

Cell morphology assessment

The medium was aspirated from the medium inlets, and the chip outlets and cells were fixed using 4% paraformaldehyde (PFA) in HBSS+ for 10 minutes at room temperature. The fixative was aspirated, and the cells were rinsed once with HBSS+. Next, the cells were permeabilized for two minutes with 0.2% Triton X-100 in HBSS+ and washed once with HBSS+. The cells were blocked in 5% BSA in HBSS+ for 30 minutes and incubated with the primary antibody solution overnight at 4°C. Mouse anti-human CD144 (1:100; 555661; BD Biosciences) was used as the primary antibodies. The wells were washed with HBSS+, followed by a one-hour incubation with Hoechst (1:2000; H3569; Invitrogen), rhodamine phalloidin (1:200; P1951; SIGMA) and the secondary antibody solution, containing an Alexa Fluor 488-conjugated goat-anti-mouse antibody (1:250; R37120; Waltham). The wells were washed three times with HBSS+. High-quality Z-stack images of the stained cells were acquired using a high-content confocal microscope (Molecular Devices, ImageXpress Micro Confocal). The orientation of the cells was determined using OrientationJ, an ImageJ plug-in, and plotted in a Rose diagram using Matlab R2015a (Mathworks).

Statistical analysis

For statistical analyses, we used IBM SPSS Statistics 23. Values are given as mean ± SEM. Multiple comparisons were made by one-way ANOVA followed by Dunnett's t-test. Results were considered significant at *P < 0.1, **P < 0.05, ***P < 0.01.

Results

Our integrated microvessel-on-a-chip platform was designed to be modular in hypoxia incubator. The platform is compatible with microfluidic culture plate, a physical sensor suite for measurement of oxygen in the microenvironment and microfluidic pump for perfusing 16

microchannels simultaneously (Figure 1a and b). The platform was contained within a custom designed XY and Z stages of Zaber Technologies (Figure 1c). The XY stage was fixed at a height of 133 mm. The Z stage was integrated with an optical fiber and probe to measure the oxygen concentration in the OrganoPlate with PyroScience Piccolo2 oxygen sensor [15]. The probe acted as a feedback to set the height of the optical fiber with the Z stage in order for the oxygen sensor to have a strong signal strength (Figure 1d). The XY and Z stages were connected to Zaber Technologies integrated controllers that could be operated together with the probe, using a set of LabView codes. The XY stage was calibrated to move to the coordinates of the desired microchannel in the microfluidic culture plate while the Z stage is automated to position the optical fiber of the oxygen sensor in correct height with our feedback control system.

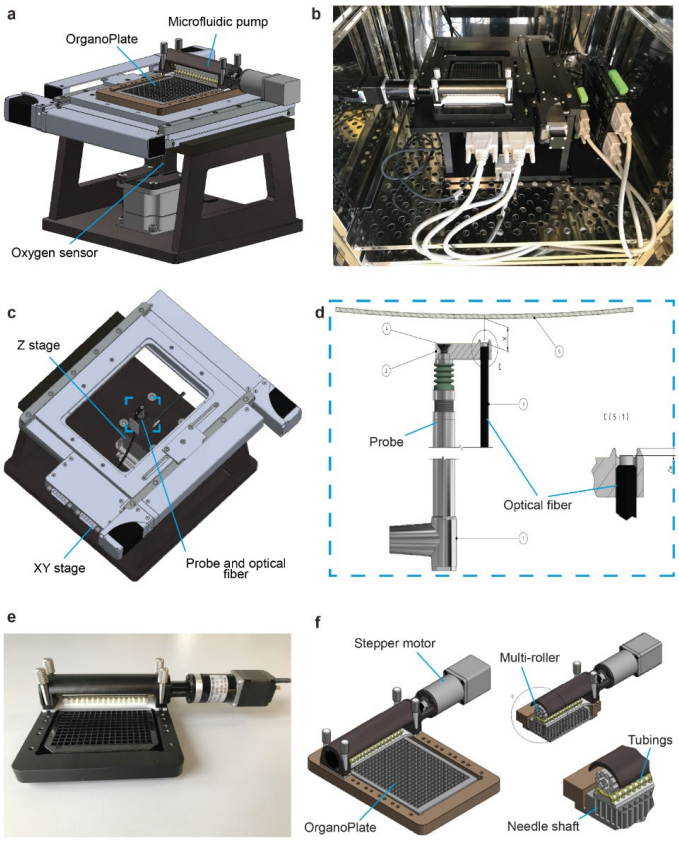

Figure 1 | Integrated automated microvessels-on-a-chip and oxygen monitoring platform. (a) Schematic of a full system where the OrganoPlate is placed on XY and Z stages with the microfluidic pump and oxygen sensor. **(b)** A photograph of the integrated platform placed in an incubator. **(c)** Top view of the integrated platform showing the oxygen sensor. The dashed rectangular box highlights the region shown in **d**. **(d)** The probe and optical fibre of the oxygen sensor. **(e)** A photograph of the microfluidic pump connected to 16 microchannels in the OrganoPlate. **(f)** Schematic diagram of the pumping system.

On top of the XY stage, the microfluidic pump was placed. This is a miniaturized, mechanically-actuated 16-channel peristaltic pump (Figure 1e and f). The small footprint of the micropump renders it portable, and allows its use on microscope stages adjacent to microfluidic devices with a 384 wells plate interface. The microfluidic pump has three core components: a multi-roller, silicon tubings (OD=2.05 mm and ID=0.25 mm) and needle shafts (OD=0.72 mm and ID=0.41 mm). A stepper motor (NEMA-11 Bipolar Stepper 28STH32), controlled with LabView,

drives the pump. As the multi-roller rotates, it compresses the tubings and pushes fluid in the direction of rotation. The number of rotations per minute (RPM) determines the flow rate.

To provide the proof-of-principle for our integrated microvessels-on-chips, we designed a novel chip structure, the rerouted 2-lane, based on the MIMETAS OrganoPlate platform. The rerouted 2-lane consists of a stratified array of 96 microfluidic chips embedded in a customized 384-well microtiter plate format that is compatible with the microfluidic pump (Figure 1e, f and 2a). Each chip contains a single microfluidic chip fixed between two layers of glass: a top plate with inlets that corresponds to the underside of selected microtiter plate wells and a bottom plate. Each chip is connected through four neighboring wells and two lanes. The flow of media is driven by the microfluidic pump from the first inlet well connected to the fourth medium outlet well through a culture lane. The second well is connected to the gel inlet for loading of extracellular matrix (ECM) lane and the fourth well is used as an observation window for monitoring the cells (Figure 2b). In the chip, microvessels were generated in the culture lane using HUVECs at the interface of collagen type 1 ECM (Figure 2c and d). The culture and ECM lanes are separated by a phaseguide, preventing the collagen from flowing into the culture lane [16].

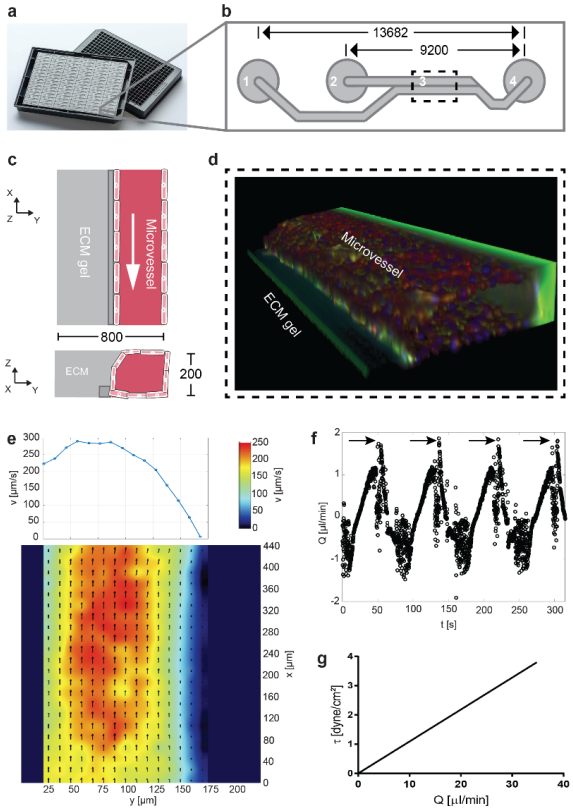

Figure 2 | Microfluidic cell culture device and operations. (a) A photograph of the rerouted 2-lane OrganoPlate. **(b)** Schematic of a single rerouted 2-lane chip; 1 = Medium inlet, 2 = Gel inlet, 3 = Observation window, 4 = Medium outlet; The dashed rectangular box highlights the region shown in **d**. **(c)** Top and side view of a microchannel interfacing with a phaseguide, ECM and culture lanes. All dimensions are in µm. **(d)** A 3D reconstruction showing the human microvessel-on-a-chip. **(e)** Measured channel cross section velocity profile. The flow regime shows some variation in velocity with parabolic trend across the channel width. **(f)** Representative flow pattern for a single microchannel. Arrows indicate point of roller release. **(g)** The channel shear stress, τ, at varying measured flow rates, Q.

VI

To investigate the flow characteristics of the ex vivo flow chamber, micro-particle image velocimetry (µPIV) experiments were conducted at several rotational speed of the microfluidic pump. We could see that the velocity distributions on the median plane of the microchannel are in accordance to theoretical velocity distribution of laminar flow in square sectional ducts except for the region near the ECM and wall [17]. This is because of the ECM and wall

roughness and the impact of particles on the surfaces (Figure 2e). The velocity was averaged on cross section, $\bar{v}$, which was then used to determine the flow rate, Q. Sudden flow rate changes occurred at the point of release of roller pins leading to slight pulsation, indicated with arrows in Figure 2f. Based on the flow rate, the shear stress, τ, in our system was determined (Figure 2g).

Shear stress controls different endothelial phenotypic characteristics [18]. To verify the use of our multi-channel microfluidic pump in 3D cell culture applications, we studied the morphology, cytoskeleton remodeling and gene expression of the microvessels-on-chips under unidirectional flow. Endothelial cells cultured in 12-well plate representing the static condition and microvessels perfused with an interval rocker platform (Perfusion rocker, MIMETAS) were taking along as controls. The interval rocker platform introduces gravitational and bidirectional flow in the microvessels-on-chips and it has been demonstrated to create functional microvessels at a 7° angle of motion and an eight-minute timed operation [19]. HUVECs were cultured in the microvessels-on-chips overnight with the interval rocker platform and this continued for additional 24h or they were put under flow for 24h with our integrated microfluidic platform set at physiological umbilical vein shear stress of 3 dyne/cm^2 and 20% oxygen. At the same time, cells were cultured in the 12-well plate to observe their morphology under static condition. At this condition, the orientation of the cells did not follow any specific trend (having the orientation angles of $0 - 90°$) and there was lots of actin stress fiber formation. In comparison, with the interval rocker platform, the cells started following the direction of the flow (corresponding to the orientation angles of $0 - 60°$), however, actin stress fiber formation was still visible. In contrary, in the presence of the microfluidic pump, the endothelial cells were highly orientated to the direction of flow with orientation angles of $0 - 30°$ and there was a decrease in stress fiber formation (Figure 3a and b). To further validate the functionality of our microfluidic pump, we looked at the impact of shear stress on regulating the shear dependent genes *Klf2* and *Klf4*. Shear stress at 0.38 dyne/cm^2 with the microfluidic pump was introduced for 24, 48 and 96h in the microvessels-on-chips. Microvessels perfused with the microfluidic pump compared with those perfused with the interval rocker and cells cultured in the 12-well plate, show significant upregulation of *Klf2* and *Klf4* (Figure 3c). In relation to the results of 0.38 dyne/cm^2, at physiological umbilical vein shear stress of 3 dyne/cm^2, we also saw an upregulation of *Klf2* and *Klf4* with the microfluidic

pump for 24h compared to cells in 12-well plate and microvessels perfused with interval rocker platform (Figure 3d). Longer time periods with 3 dyne/cm^2 could not be measured, due to an increase in endothelial cell death.

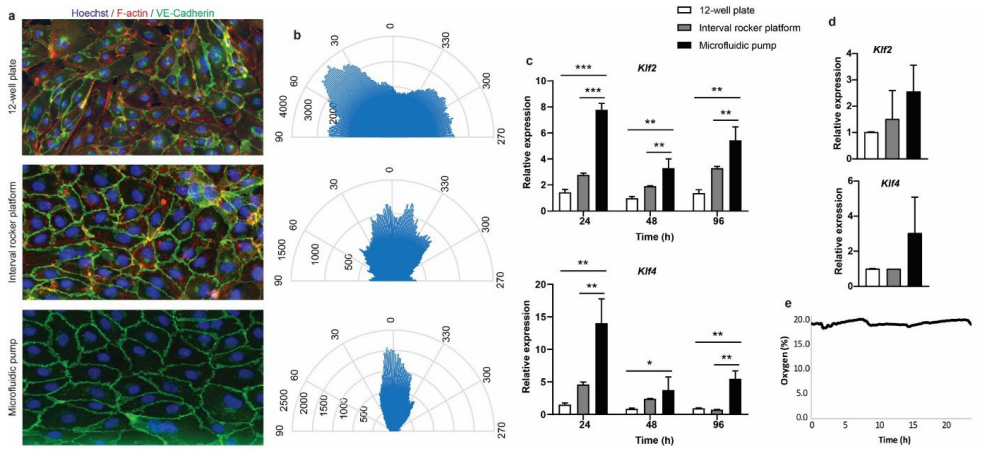

Figure 3 | Effects of flow on remodelling of the cytoskeleton in endothelial cells. HUVECs were cultured in 12-well plate representing the static condition, microvessels-on-chips were perfused with an interval rocker platform (Perfusion rocker, MIMETAS) and microfluidic pump. The interval rocker platform was set at a 7° angle of motion and an eight-minute timed operation to allow continuous bidirectional flow of medium in the microvessels. The microfluidic pump allowed unidirectional flow of medium in the microvessels. **(a-b)** Fluorescent images of cells with corresponding Rose plot of HUVEC alignment suggest that endothelial cells cultured in 12-well plate and microvessels-on-chips perfused with the interval rocker platform are more randomly orientated, whereas microvessels-on-chips perfused with the microfluidic pump with a shear stress of 3.0 dyne/cm^2 are uniformly orientated and aligned in one direction. **(c)** Shear stress of 0.38 dyne/cm^2 introduced with microfluidic pump in the microvessels for 24, 48 and 96h resulted in increased *Klf2* and *Klf4* expression. **(d)** Shear stress of 3.0 dyne/cm^2 introduced with the microfluidic pump in the microvessels for 24h resulted in increased *Klf2* and *Klf4* expression. Data are presented as mean and s.e.m; n = 2. **(e)** Continual measurement of oxygen within the integrated microvessels-on-chips.

Since, the integrated microvessels-on-chips platform is a fully closed system, the oxygen concentration was constantly monitored in order to be sure of gas permeability. The relatively stable oxygen levels observed in Figure 3e could be attributed to the gas permeability of the silicon tubings of the microfluidic pump. Interestingly, it takes the oxygen level in the

microfluidic device about 17h to reach steady state after the incubator has been set to 3.4% O_2 (Supplementary Figure 1). This has important implications for carrying out hypoxia studies in the future. Taken together, these results suggest that the integrated microvessels-on-a-chip platform induces flow dynamics that has an effect on the morphology of the endothelial cells. This is connected to the change in the mechanically induced signaling related to change in gene expression.

Discussion

In this article, we describe the design, fabrication and performance of a 16-channel peristaltic micropump for timed routing of fluids to interface physical sensor for monitoring oxygen. We used microvessels in the OrganoPlate as a working example to test the micropump. The sensing was performed *in situ* in an uninterrupted and automated manner, allowing for long-term monitoring of oxygen.

Various pumps have been developed to induce flow for microfluidic applications, but only very few are multi-channel pumps [20]. Multi-channel pumping can save time and resources to carry out large scale drug screening. Recent reports have addressed the need to create microfluidic pumping systems that are portable and can be integrated with other devices [10, 14]. Our system is rendered suitable since the pump approaches dimensions of microfluidic devices.

In this study, we show that flow has an effect on the morphology and cytoskeleton of the endothelial cells. The *in vivo* umbilical vein shear stress has been characterized to be as low as 3 dyne/cm^2 [21]. Considering this shear stress value under unidirectional flow, induced by our microfluidic pump, endothelial cells were more aligned to the direction flow in comparison to bidirectional flow with the interval rocker platform and cells cultured in 12-well plate [18]. Furthermore, the microvessels exhibited a change in the expression of proteins that are known to play significant roles in regulating shear-sensitive endothelial functions, such as inflammation, oxidative stress and angiogenesis [11]. These observations demonstrated the suitability of the presented microfluidic pumping system for studying the effect of flow on the biology of endothelial cells *in vivo*.

Meanwhile, we acknowledge several limitations of our current integrated microfluidic multi-channel pumping system. We could introduce shear stress of 3 dyne/cm^2 with our microfluidic pump for 24h, longer periods lead to increased cell death and instability of the microvessels. This observation may be explained by the fact that there is some degree of back pressure and pulsation in the system, which can effect cell viability after a long period of time [22]. Moreover, the channel wall is rigid and this condition is not met in reality, because the microvessels *in vivo* are distensible and their diameter changes with fluidic pressure [23]. Although flow characteristics are not superior to syringe pumps, the microfluidic pump design offers many advantages. The interface of liquids to and from the pump is completed without requiring excessive tubings, but via needle shafts in the inlets and outlets of the OrganoPlate. This miniaturizes the whole set-up of the system and reduces pump dead volumes. Furthermore, the microfluidic pump with the OrganoPlate fits on microscope stages, allowing unobstructed microscopic observation during perfusion.

The microfluidic pump can only perfuse 16 microvessels in parallel. Effort is being made to perfuse 96 microvessels, thereby covering the whole OrganoPlate and further improving the microfluidic pump for high-throughput perfusion [19]. Additionally, it is realized that the current platform requires manual sampling in the microvessels-on-chips. Further work is required to integrate an automated sampling system in order to achieve a long-lasting, self-assembled microvascular network without temporal exposure to the out-side environment.

Conflict of interest

Authors declare no conflict of interest related to the content of this manuscript. T.H. is shareholder in Mimetas BV, which was involved in the fabrication of the chips used in this study.

Acknowledgements

This study was financially supported by the RECONNECT CVON Groot consortium, which is funded by the Dutch Heart Foundation. AJ and TH, AJvZ were supported by a ZonMW MKMD

grant (114022501). AM and TH acknowledge the support by the NWO-TTW (IMMUNMET, grant number 16249). TH acknowledge the support by the TKI METABOCHIP project.

References

1. Organization, W.H. *Cardiovascular Diseases*. [cited 2019 19-08-2019]; Available from: https://www.who.int/health-topics/cardiovascular-diseases/.

2. Owan, T.E., et al., *Trends in prevalence and outcome of heart failure with preserved ejection fraction.* N Engl J Med, 2006. **355**(3): p. 251-9.

3. Paulus, W.J. and C. Tschope, *A novel paradigm for heart failure with preserved ejection fraction: comorbidities drive myocardial dysfunction and remodeling through coronary microvascular endothelial inflammation.* J Am Coll Cardiol, 2013. **62**(4): p. 263-71.

4. Lam, C.S.P. and D.L. Brutsaert, *Endothelial Dysfunction A Pathophysiologic Factor in Heart Failure With Preserved Ejection Fraction.* Journal of the American College of Cardiology, 2012. **60**(18): p. 1787-1789.

5. Savoji, H., et al., *Cardiovascular disease models: A game changing paradigm in drug discovery and screening.* Biomaterials, 2019. **198**: p. 3-26.

6. Duval, K., et al., *Modeling Physiological Events in 2D vs. 3D Cell Culture.* Physiology (Bethesda), 2017. **32**(4): p. 266-277.

7. Rasheena, E., et al., *Three-Dimensional Cell Culture Systems and Their Applications in Drug Discovery and Cell-Based Biosensors.* ASSAY and Drug Development Technologies, 2014. **12**(4): p. 207-218.

8. Benam, K.H., et al., *Small airway-on-a-chip enables analysis of human lung inflammation and drug responses in vitro.* Nat Methods, 2016. **13**(2): p. 151-7.

9. Marturano-Kruik, A., et al., *Human bone perivascular niche-on-a-chip for studying metastatic colonization.* Proc Natl Acad Sci U S A, 2018. **115**(6): p. 1256-1261.

10. Zhang, Y.S., et al., *Multisensor-integrated organs-on-chips platform for automated and continual in situ monitoring of organoid behaviors.* Proc Natl Acad Sci U S A, 2017. **114**(12): p. E2293-E2302.

11. Ajami, N.E., et al., *Systems biology analysis of longitudinal functional response of endothelial cells to shear stress.* Proceedings of the National Academy of Sciences, 2017. **114**(41): p. 10990-10995.

12. Liu, M.C., et al., *Electrofluidic pressure sensor embedded microfluidic device: a study of endothelial cells under hydrostatic pressure and shear stress combinations.* Lab Chip, 2013. **13**(9): p. 1743-53.

13. Maoz, B.M., et al., *Organs-on-Chips with combined multi-electrode array and transepithelial electrical resistance measurement capabilities.* Lab Chip, 2017. **17**(13): p. 2294-2302.

14. Junaid, A., et al., *An end-user perspective on Organ-on-a-Chip: Assays and usability aspects.* Current Opinion in Biomedical Engineering, 2017. **1**: p. 15-22.

15. Ehgartner, J., et al., *Online analysis of oxygen inside silicon-glass microreactors with integrated optical sensors.* Sensors and Actuators B-Chemical, 2016. **228**: p. 748-757.

16. Vulto, P., et al., *Phaseguides: a paradigm shift in microfluidic priming and emptying.* Lab Chip, 2011. **11**(9): p. 1596-602.

17. Wang, H. and Y. Wang, *Measurement of water flow rate in microchannels based on the microfluidic particle image velocimetry.* Measurement, 2009. **42**(1): p. 119-126.

18. Tovar-Lopez, F., et al., *A Microfluidic System for Studying the Effects of Disturbed Flow on Endothelial Cells.* Frontiers in Bioengineering and Biotechnology, 2019. **7**(81).

19. van Duinen, V., et al., *96 perfusable blood vessels to study vascular permeability in vitro.* Sci Rep, 2017. **7**(1): p. 18071.

20. Skafte-Pedersen, P., et al., *Multi-channel peristaltic pump for microfluidic applications featuring monolithic PDMS inlay.* Lab Chip, 2009. **9**(20): p. 3003-6.

21. Saw, S.N., et al., *Characterization of the in vivo wall shear stress environment of human fetus umbilical arteries and veins.* Biomech Model Mechanobiol, 2017. **16**(1): p. 197-211.

22. Wang, F., et al., *Oscillating flow promotes inflammation through the TLR2–TAK1–IKK2 signalling pathway in human umbilical vein endothelial cell (HUVECs).* Life Sciences, 2019. **224**: p. 212-221.

23. Katritsis, D., et al., *Wall shear stress: theoretical considerations and methods of measurement.* Prog Cardiovasc Dis, 2007. **49**(5): p. 307-29.

24. Santiago, J., et al., *A particle image velocimetry system for microfluidics. Exp Fluid.* Experiments in Fluids, 1998. **25**: p. 316-319.

25. Meinhart, C., S. T. Wereley, and J. Santiago, *PIV measurements of a microchannel flow.* Experiments in Fluids, 1999. **27**: p. 414-419.

Supplementary Figures

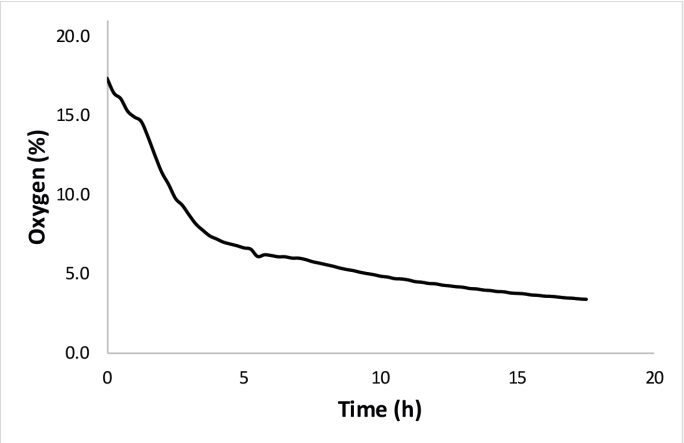

Supplementary Figure 1 | Continual measurement of oxygen within the integrated microvessels-on-chips after the incubator was set to 3.4% O_2.